NIH Public Access
Author Manuscript
J Immunol. Author manuscript; available in PMC 2013 October 28.

Published in final edited form as:
J Immunol. 2011 February 15; 186(4): . doi:10.4049/jimmunol.1003225.

Basal and Antigen-Induced Exposure of the Proline-Rich Sequence in CD3ε

Javier de la Cruz[*,†], **Travis Kruger**[*,‡], **Christopher A. Parks**[*,‡], **Robert L. Silge**[§], **Nicolai S. C. van Oers**[§], **Immanuel F. Luescher**[¶], **Adam G. Schrum**[*], and **Diana Gil**[*]

[*]Department of Immunology, College of Medicine, Mayo Clinic, Rochester, MN 55905 [†]Initiative to Maximize Student Diversity and Post Baccalaureate Research Education Program, College of Medicine, Mayo Clinic, Rochester, MN 55905 [‡]Summer Undergraduate Research Fellowship Program, College of Medicine, Mayo Clinic, Rochester, MN 55905 [§]Department of Immunology, University of Texas Southwestern Medical Center, Dallas, TX 75390 [¶]Ludwig Institute for Cancer Research, Lausanne Branch, University of Lausanne, 1066 Epalinges, Switzerland

Abstract

The CD3ε cytoplasmic tail contains a conserved proline-rich sequence (PRS) that influences TCR–CD3 expression and signaling. Although the PRS can bind the SH3.1 domain of the cytosolic adapter Nck, whether the PRS is constitutively available for Nck binding or instead represents a cryptic motif that is exposed via conformational change upon TCR–CD3 engagement (CD3Δc) is currently unresolved. Furthermore, the extent to which a *cis*-acting CD3ε basic amino acid-rich stretch (BRS), with its unique phosphoinositide-binding capability, might impact PRS accessibility is not clear. In this study, we found that freshly harvested primary thymocytes expressed low to moderate basal levels of Nck-accessible PRS ("open-CD3"), although most TCR–CD3 complexes were inaccessible to Nck ("closed-CD3"). Ag presentation in vivo induced open-CD3, accounting for half of the basal level found in thymocytes from MHC^+ mice. Additional stimulation with either anti-CD3 Abs or peptide–MHC ligands further elevated open-CD3 above basal levels, consistent with a model wherein antigenic engagement induces maximum PRS exposure. We also found that the open-CD3 conformation induced by APCs outlasted the time of ligand occupancy, marking receptors that had been engaged. Finally, CD3ε BRS–phosphoinositide interactions played no role in either adoption of the initial closed-CD3 conformation or induction of open-CD3 by Ab stimulation. Thus, a basal level of open-CD3 is succeeded by a higher, induced level upon TCR–CD3 engagement, involving CD3Δc and prolonged accessibility of the CD3ε PRS to Nck.

The TCR is a heterodimer composed of α and β subunits (or γ and δ in γδ T cells) that binds specifically to Ags in the form of peptides presented by MHC on the surfaces of APCs. Although the TCR lacks an intrinsic capacity to transduce signals to the cytoplasm, it is noncovalently associated with the CD3 complex, a group of four transmembrane proteins (CD3ε, γ, δ, and ζ). These proteins have long cytoplasmic tails that each contain one or multiple copies of the ITAM (1). TCR engagement by peptide–MHC (pMHC) ligands induces phosphorylation of CD3 ITAMs by src-family tyrosine kinases (1). However, prior

Copyright © 2011 by The American Association of Immunologists, Inc. All rights reserved.

Address correspondence and reprint requests to Diana Gil, Department of Immunology, College of Medicine, Mayo Clinic, 321 Guggenheim Building, 200 First Street SW, Rochester, MN 55905. gilpages.diana@mayo.edu.

Disclosures
The authors have no financial conflicts of interest.

NIH-PA Author Manuscript
NIH-PA Author Manuscript
NIH-PA Author Manuscript

NIH-PA Author Manuscript

NIH-PA Author Manuscript

NIH-PA Author Manuscript

to ITAM phosphorylation, the precise mechanism(s) by which the TCR initially communicates the event of Ag recognition to the CD3 complex is incompletely understood (2).

Among several nonexclusive models, conformational change of TCR–CD3 has been proposed as a mechanism that might confer Ag recognition (3, 4). Using a biochemical approach, it was reported that TCR engagement induced the exposure of what appeared to be a cryptic proline-rich sequence (PRS) in the CD3ε cytoplasmic tail, a sequence that can mediate the interaction of CD3ε with the SH3.1 domain of the cytoplasmic adapter protein Nck (5). At the time, PRS exposure was interpreted to result from a conformational change in CD3 (CD3Δc) because it occurred prior to and independent of ITAM phosphorylation. Subsequent studies showed that CD3Δc was inducible by either anti–TCR–CD3 Abs or cognate pMHC ligands, irrespective of whether thymocytes were stimulated with selection ligands or mature T cells were stimulated with antigenic ligands (6–8). In absence of comprehensive structural information, the PRS-accessible CD3 conformation was termed “open-CD3” and the PRS-inaccessible conformation “closed-CD3” (6). Using soluble ligands including pMHC tetramers, one study showed that the open and closed CD3 conformations were instantaneously reversible, open-CD3 being adopted upon ligation and reverting to closed-CD3 upon ligand dissociation (9).

Originally implicated in synapse formation and T cell activation (5), the function of the CD3ε PRS has subsequently been studied in greater detail. Whereas initial studies using polyclonal retrogenic mice showed no apparent difference between PRS wild-type versus mutant-bearing T cells (10), retrogenic mice expressing mutant PRS associated with certain TCR clonotypes have shown this sequence is required to amplify signals from weak pMHC ligands (11). More recently, the use of transgenic mice has shown defects in responsiveness to weak TCR ligands and in the positive selection of thymocytes deficient for the PRS (12). In another study, where the induction of conformational change was isolated as a single variable and PRS exposure was monitored as evidence of CD3Δc, both open-CD3 and receptor aggregation were shown to be required for optimal T cell signaling (9). Taken together, the PRS is thought to play an important role in TCR–CD3 receptor biology by functioning in concert with other signaling sequences and mechanisms that collectively respond to antigenic engagement.

However, some recent work has called into question several critical elements of the conformational model described above. One group reported that in C57BL/6 (B6) wild-type (WT) thymocytes, the CD3ε PRS seemed constitutively exposed, and anti-CD3 stimulation did not significantly increase open-CD3 (12). PRS deficiency was shown to correlate with increased TCR–CD3 expression, implying that the PRS controls constitutive expression of the receptor in double-positive (DP) thymocytes. Independent work has since corroborated the role of the CD3ε PRS in regulating TCR–CD3 ubiquitylation and expression in DP thymocytes while additionally demonstrating PRS activity in promoting proliferation of double-negative thymocytes (13–16). Considering all studies together, it is currently not clear whether the initial interpretation that CD3Δc is required to induce PRS accessibility is correct, whether thymocytes are unique by expressing the PRS in a constitutively accessible conformation, or whether differences in experimental systems account for the discrepant observations (17). Because it is agreed that the CD3ε PRS is functionally relevant to TCR–CD3 expression and the efficiency of thymic development, the issue of whether this sequence is constitutively versus inducibly accessible to Nck is currently considered a significant outstanding question in the field of TCR triggering (2).

A second recently described cytoplasmic motif of CD3ε may also be implicated in TCR signaling, possibly involving CD3Δc. A basic amino acid-rich stretch (BRS) in the

NIH-PA Author Manuscript

NIH-PA Author Manuscript

NIH-PA Author Manuscript

juxtamembrane region of the CD3ε cytoplasmic tail can mediate interaction with select phosphoinositides that are present at different locations in the cell including the inner leaflet of the plasma membrane (18, 19). One study showed that upon membrane interaction, the tyrosines of the CD3ε ITAM were bound to the nonpolar phase of the lipid bilayer, inaccessible to src kinases (18). Because the capacity to interact with phospholipids is shared with CD3ζ (20, 21), it has been proposed that TCR engagement might result in the release of membrane-sequestered CD3 ITAMs from the lipid bilayer to facilitate their phosphorylation (2, 18, 22, 23). Two possibilities have been suggested that might achieve this: i) mobilization of engaged TCR–CD3 to a different, non-CD3-binding lipid microenvironment (18, 22) or ii) CD3 conformational change to move CD3 tails from the membrane to the cytoplasm (2, 23). Because open-CD3 has been proposed to result from such a conformational change, perhaps the CD3ε BRS, by interacting with the plasma membrane, may be required to conceal the PRS in the absence of receptor engagement.

In the current work, we have focused on clarifying the extent to which PRS accessibility to Nck is influenced by constitutive expression, TCR–CD3 engagement, and the CD3ε BRS motif. Several different experimental systems have been used to resolve these issues and provide explanations, where possible, as to the reasons why some previous data appeared to conflict. This work now allows both previous and new results to be resolved into an updated model of how TCR–CD3 and pMHC ligands together control CD3Δc and PRS accessibility to Nck. We propose that this model contributes to our understanding of the initial Ag recognition events associated with TCR triggering.

Materials and Methods

DNA constructs and mice

The construct pGEX-4T1-GST-SH3.1α (SH3.1 derived from human Nck-α) was kindly provided by Dr. R. Geha (Children's Hospital, Harvard Medical School, Boston, MA). B6 mice were purchased from The Jackson Laboratory. B6 mice deficient for MHC class II β-chain and β_2-micro-globulin ($Abb^{-/-}$ $\beta 2m^{-/-}$) were purchased from Taconic. Mice transgenic for CD3ε BRS WT or CD3ε BRS-Substitute have been previously described (19), having been bred to the $CD3\varepsilon^{-/-}$ background (24). OT-I $Rag^{-/-}$ $\beta 2m^{-/-}$ mice were kindly provided by Terry Potter (National Jewish Health, Denver, CO). All mice were used between 6 and 12 wk of age. Mouse procedures were approved by the Mayo Institutional Animal Care and Use Committee and are consistent with National Institutes of Health guidelines for the care and use of animals.

Abs and other reagents

The mAb anti-CD3ζ (H146) was kindly provided by Ed Palmer (University Hospital-Basel, Basel, Switzerland). The rabbit serum anti-MHC class I (α-P8) was kindly provided by Hidde L. Ploegh (Whitehead Institute for Biomedical Research, Massachusetts Institute of Technology, Cambridge, MA). The mAb anti-Vα2 was purified from supernatant of the hybridoma B20.1. Abs from BD Biosciences included anti-TCRβ (H57), anti-Thy1.2 (53-2.1), anti-CD4 (RM4-5), anti-CD8α (53.6.7), anti-CD69 (H12F3), anti-CD3ε (2C11), and anti–H2-K^d (SF1-1.1). Monoclonal anti-CD3ε APA1/1 was obtained in purified, unconjugated form from GE Biosciences, PE-labeled from BD, and Alexa Fluor (AF)-555 labeled from Upstate Biotech. Other reagents included serum ham IgG control (Jackson ImmunoResearch), streptavidin AF-488 and AF-647 (Invitrogen), True Stain FcX (Biolegend), GSH Sepharose and protein G Sepharose (GE Biosciences), goat serum (Sigma Chemical), Brij-58 (Sigma Chemical), and Digitonin (Sigma Chemical).

NIH-PA Author Manuscript

NIH-PA Author Manuscript

NIH-PA Author Manuscript

Cell lines and peptide loading

The T1.4 $CD8^+$ hybridoma expresses the T1 TCR specific for the H-$2K^d$ restricted peptide from *Plasmodium berghei* (PbCs 252–260: SYIPSAEKI) chemically conjugated with photoreactive 4-azidobenzoic acid (ABA) (25, 26). The peptide PbCs 252–260-ABA (pSYIP) was produced following protocols described elsewhere (26). The murine mastocytoma P815 (American Type Culture Collection) expresses H-$2K^d$ and was used as APC for T1 hybridoma cells. T2-K^b cells [kindly provided by T. Potter (27)], express H-$2K^b$ and were used as APCs for OT-I cells. The H2-K^b restricted peptides pFARL (SSIEFARL) and pOVA (SIINFEKL) were purchased from Elim Biopharmaceuticals. All peptides were loaded at 2 μM into their respective APCs for 2 h. After loading, APCs were washed once to remover excess peptide prior to coculture with thymocytes.

Thymocyte stimulation

When mouse thymocytes were stimulated with soluble Abs to induce open-CD3, cells were preincubated on ice with 10 μg/ml of either hamster IgG isotype control (Ham IgG) or anti-CD3 Ab (2C11) in RPMI medium supplemented with 5% FBS for 10 min and then incubated for 15 min at 37°C. Stimulation was stopped by sample centrifugation at 4°C followed by lysis of pelleted cells. Alternatively, thymocytes were lysed prior to induction of open-CD3 with soluble Abs. In this case, 10 μg/ml of either Ham IgG or 2C11 were added to the postnuclear fractions of thymocytes at the preclearing step of the CD3 pull-down assay. OT-I $Rag^{-/-}$ $\beta 2m^{-/-}$ thymocytes and T1 hybridoma cells were stimulated with peptide-loaded T2-K^b and P-815 APCs, respectively. In this case, both T cells and peptide-loaded APCs were cocultured in a ratio of 1:1 for 30 min at 37°C to induce open-CD3. Immediately after stimulation, cocultures were centrifuged at 4°C followed by lysis of pelleted cells.

CD3 pull-down assay, immunoprecipitation, and Western blot

The CD3 pull-down (CD3-PD) assay was previously described as a means to detect open-CD3 conformation (5, 6). Briefly, cells were lysed on ice for 30 min using isotonic buffer containing non-ionic detergents (either 0.3% Brij 58 or 1% Digitonin), and postnuclear lysates were obtained. A one-tenth fraction of each postnuclear lysate was mixed with an equal volume of acetone, and the resulting protein precipitates were used to represent the total CD3 content in each sample (total lysate; TL) by Western blot (WB) for CD3 ζ (H146). The remainder of each sample was precleared by incubation with GST beads (1 h, 4°C) prior to specific pull-down with GST-SH3.1 beads (4–12 h, 4°C), followed by SDS-PAGE, nitrocellulose transfer, and WB for CD3 ζ (H146). Where indicated, APA1/1 was added to samples during the preclearing step to act as competitive inhibitor of the specific CD3 pull-down with GST-SH3.1 beads (6) to establish the background open-CD3 detection associated with this assay. For immunoprecipitation, postnuclear lysates prepared as described above were incubated with protein G Sepharose beads coupled with Ab during 4–12 h at 4°C. Then beads were washed extensively and subjected to SDS-PAGE, nitrocellulose transfer, and WB.

Quantification of open-CD3 conformation

The pixels of CD3ζ bands detected by WB in TL and CD3-PD samples were counted using the Threshold function and the Magic Wand tool in Adobe Photoshop Elements. Lightest exposures where weakest bands were detectable were used to count pixels. Threshold was set such that every band counted was detected as a well-defined single element. A CD3-PD/TL ratio of pixels was calculated for each sample to determine its content of open-CD3 relative to its total amount of CD3. Basal open-CD3 was calculated as a fold-increase over open-CD3 found as background of the CD3-PD assay. The induction of open-CD3 by anti-

NIH-PA Author Manuscript

NIH-PA Author Manuscript

NIH-PA Author Manuscript

CD3 stimulation was calculated as a fold-increase over the amount of open-CD3 observed in nonstimulated samples. For statistical analysis, five or more independent experiments were performed, and the central and variance values (arithmetic mean, median, SD, SE) of basal and stimulated open-CD3 were calculated. Paired *t* tests were run to calculate *p* values to examine possible differences between experimental groups.

Intracellular staining of CD3ε cytoplasmic tail with the mAb APA1/1

Thymocytes from either B6 or Abb$^{-/-}$ β2m$^{-/-}$ mice were stained with anti-Thy1.2–allophycocyanin, washed extensively, and stimulated with soluble Abs as described earlier.

To provide an in internal negative control for CD3 staining, splenocytes from Abb$^{-/-}$ β2m$^{-/-}$ mice, prestained with anti-Thy1.2–PercCP and extensively washed, were added to both types of thymocyte samples. Next, mixtures of thymocytes and splenocytes were fixed and permeabilized with 10 volumes of Cytofix/Cytoperm kit (BD) for 60 min on ice. Samples were washed once and resuspended in a blocking buffer consisting of washing buffer from the Cytofix/Cytoperm kit supplemented with 5% goat serum and True Stain FcX at 5 μg/ml. Samples were blocked overnight on ice, washed once, and stained for 45 min on ice with APA1/1–PE (BD) diluted in a range from 1:2 to 1:1024 in the blocking buffer. Then, samples were washed twice, and cells were analyzed on a BD FACSCalibur flow cytometer calibrated with RCP-30-5A beads (Spherotech). For confocal microscopy analysis of APA1/1 staining, OT-I Rag$^{-/-}$ β2m$^{-/-}$ thymocytes were stimulated for 30 min at 37°C with 5 μm polystyrene latex beads [No. 2-5000; Interfacial Dynamics(28)] that had been covalently coupled with anti-Vα2 Ab. Stimulation was stopped by adding 10 volumes of ice-cold Cytofix/Cytoperm kit (BD) to the mixture of cells and beads. Then, samples were immediately placed on ice and incubated for 60 min. After the fixation/permeabilization step, samples were washed and blocked as described earlier for flow cytometry. To provide an internal control for low-level CD3 staining to be compared with stimulated OT-I thymocytes, samples were mixed with nonstimulated thymocytes from Abb$^{-/-}$ β2m$^{-/-}$ mice that had been fixed, permeabilized, and blocked in parallel. The resulting samples were stained for 45 min on ice with APA1/1–AF-555 diluted 1:250 in the blocking buffer. Then, samples were washed twice, mixed with ProLong Gold (Invitrogen), and mounted onto coverslips for confocal analysis. Samples were imaged on a Zeiss LSM-510 confocal microscope. Images were analyzed using ImageJ software.

Results

TCR–CD3 engagement induces open-CD3 in B6 thymocytes

To determine the extent to which TCR–CD3 engagement affects the exposure of the CD3ε PRS, B6 thymocytes were treated in vitro with either Ham IgG or anti-CD3ε mAb 2C11 in 22 independent experiments. After stimulation, thymocytes were lysed and postnuclear fractions subjected to the CD3-PD assay, in which the SH3.1 domain of Nck, immobilized to Sepharose beads, captures TCR–CD3 complexes containing Nck-accessible CD3ε PRS (open-CD3) (5, 6). The quantity of open-CD3 induced by anti-CD3 stimulation was calculated relative to the amount of open-CD3 found in nonstimulated thymocytes. We observed that anti-CD3 stimulation induced increased open-CD3 in all experiments, but the intensity of this induction was variable. Representative low, intermediate, and high fold-inductions of open-CD3 found among our experiments are shown in Fig. 1*A*–*C*. Over all experiments, open-CD3 induction ranged from a minimum value of 1.9-fold to a maximum of 11.5-fold (mean = 4.7, median = 4.4, SD = 2.5, SE = 0.5; Fig. 1*D*). We conclude that engagement of the TCR–CD3 complex consistently increases the level of open-CD3 in B6 thymocytes, although this inducibility displays some variance between experiments.

NIH-PA Author Manuscript

NIH-PA Author Manuscript

NIH-PA Author Manuscript

Nonstimulated B6 thymocytes express basal levels of open-CD3

In the experiments described above, a lower initial level of open-CD3 seemed to be readily detectable from thymocytes without overt experimental TCR–CD3 engagement (Fig. 1*A*–*C*). We wished to determine whether this apparent open-CD3 was attributable to assay background (nonspecific CD3 appearing in the pull-down) or true basal expression (specific PRS-dependent CD3 binding to SH3.1). To distinguish between these two possibilities, we used the mAb APA1/1, which binds an amino acid sequence in CD3ε that partially overlaps with the PRS (29), blocking and outcompeting binding to SH3.1 (5, 6). Therefore, any CD3 present in pull-downs performed in the presence of APA1/1 must be independent of the CD3ε PRS, revealing nonspecific assay background. In 12 independent experiments, we consistently found that basal open-CD3 was higher than the assay background, and additionally anti-CD3 treatment induced yet greater open-CD3 levels (Fig. 2*A*, 2*B*). These trends were evident whether the data were analyzed relative to the assay background (Fig. 2*B*, 2*C*) or relative to the positive basal level (Fig. 2*A*). We conclude that freshly isolated B6 thymocytes contain basal levels of open-CD3 expressed in the absence of overt stimulation. Additionally, upon in vitro TCR–CD3 engagement, increased levels of open-CD3 are induced (Fig. 2*C*).

Thymic Ag presentation induces basal open-CD3 in WT thymocytes in vivo

To determine the impact on basal open-CD3 of thymocyte interactions with self-pMHC ligands, we compared thymocytes from B6 WT and Abb$^{-/-}$ β2m$^{-/-}$ mice. Thymocytes from the latter cannot engage with Ags due to MHC deficiency (30). CD3-PD experiments were designed as above, with assay background, basal, and stimulated open-CD3 levels observed and quantified. As seen above, anti-CD3 stimulation increased the amount of open-CD3 relative to basal conditions in both WT and Abb$^{-/-}$ β2m$^{-/-}$ thymocytes (Fig. 3*A*). However, we found that B6 WT displayed a lower fold-induction of stimulated relative to basal open-CD3 compared with that of B6 Abb$^{-/-}$ β2m$^{-/-}$ thymocytes. Notably, this difference was not due to differences in stimulated open-CD3 between WT and knockout thymocytes, but rather to differences in the basal levels of the two groups: relative to the assay background, B6 WT thymocytes displayed higher basal open-CD3 than B6 Abb$^{-/-}$ β2m$^{-/-}$ thymocytes (WT = 5.14, Abb$^{-/-}$ β2m$^{-/-}$ = 2.74; Fig. 3*A*). In contrast, the maximal open-CD3 induced by anti-CD3 treatment was roughly equivalent (WT = 10.2, Abb$^{-/-}$ β2m$^{-/-}$ = 10.9; Fig. 3*A*). To compare data generated in five independent experiments, we considered anti-CD3 treatment as a maximal open-CD3 condition and analyzed basal open-CD3 as a percentage of this maximum (Fig. 3*A*, 3*B*, % Max. of Stimulated). We found that while WT thymocytes expressed ~40% maximum basal open-CD3 in these experiments, the absence of MHC expression reduced basal open-CD3 by approximately half (Fig. 3*B*). Therefore, the reason why anti-CD3 produced less fold-induction of open-CD3 in WT versus Abb$^{-/-}$ β2m$^{-/-}$ thymocytes (Fig. 3*C*) was because the freshly harvested basal level in WT was already closer to the maximum, having been increased in vivo by an MHC-dependent mechanism. These data demonstrate that MHC expression increases thymocyte display of the open-CD3 conformation, arguing that engagement of TCR by thymic Ag presentation induces open-CD3 in vivo.

The mAb APA1/1 can bind to the CD3ε cytoplasmic tail independently of TCR–CD3 engagement

A second method has been published as a means to detect open-CD3 in intact cells: it involves the use of the mAb APA1/1 to specifically stain open but not closed CD3 (7, 8, 11, 12). Because some studies have relied on this method, we tested whether accessibility of APA1/1 to its CD3ε epitope for intracellular staining mimicked the accessibility of the PRS to SH3.1 in the CD3-PD assay. We compared the two assays in parallel assessing the B6 WTand Abb$^{-/-}$ β2m$^{-/-}$ samples described above. Unexpectedly, we found that

NIH-PA Author Manuscript

NIH-PA Author Manuscript

NIH-PA Author Manuscript

nonstimulated thymocytes from both mice showed equivalent intracellular APA1/1 staining, regardless of the dilution of APA1/1 used in the assay (Fig. 4*A*–*C*). This result was in contrast to that of the CD3-PD assay (Fig. 3*A*), where stimulation was shown to induce open-CD3. All thymocyte stainings with APA1/1 were compared with that of non-T cell splenocytes that had been added to each sample prior to the staining procedure, confirming that APA1/1 behaved as a T cell-specific probe (Fig. 4*A*). Therefore, in these experiments, APA1/1 was unable to distinguish open from closed CD3 and rather stained both nonstimulated and stimulated CD3 complexes equivalently.

We also tested by confocal microscopy whether APA1/1 displayed specificity for engaged TCR–CD3 complexes. We isolated preselection DP thymocytes from OT-I $Rag^{-/-}$ $\beta2m^{-/-}$ mice (31) that were previously shown to undergo CD3Δc upon TCR stimulation (6). These thymocytes were labeled on ice with anti-Thy1.2 and mixed in a 1:4 ratio with anti-Vα2–coupled polystyrene latex beads, which can bind the $V\alpha2^{+}$ OT1 TCR. Samples were incubated 30 min at 37°C, followed by addition of ice-cold fixation/permeabilization solution in excess to halt the stimulation. Next, unlabeled, fixed/permeabilized $Abb^{-/-}$ $\beta2m^{-/-}$ thymocytes were added to samples to allow comparison of their low basal open-CD3 with the open-CD3 found in the bead-stimulated OT-I thymocytes. Bead-stimulated OT-I $Rag^{-/-}$ $\beta2m^{-/-}$ thymocytes were identified by the colocalization and concentration of both APA1/1 (marking CD3ε) and anti-Thy1.2 mAb [marking lipid rafts through this GPI-linked protein (32)] toward the associated bead (Fig. 4*D*, *right panels*). We found that not only bead-stimulated thymocytes but also nonstimulated $Abb^{-/-}$ $\beta2m^{-/-}$ and bead-unassociated OT-I $Rag^{-/-}$ $\beta2m^{-/-}$ thymocytes displayed a positive APA1/1staining at the plasma membrane (Fig. 4*D*, *left* and *central panels*). We conclude that whereas the CD3-PD assay specifically detects open-CD3, the APA1/1 staining assay as we have performed it detects the CD3 complex regardless of TCR–CD3 engagement.

Open-CD3 outlasts TCR engagement by APCs

It was previously shown that open-CD3 induced by soluble TCR–CD3 ligands spontaneously reverts to the closed conformation upon detachment of the stimulus from the receptor (9). We wished to determine whether the open-CD3 induced by APCs displayed this property or alternatively whether APC engagement was capable of stabilizing open-CD3 after ligand dissociation. Because we had detected the induction of open-CD3 by APCs in OT-I $Rag^{-/-}$ $\beta2m^{-/-}$ thymocytes in the past (6, 33), we used this system to test whether MHC ligands would coprecipitate with open-CD3 in the CD3-PD assay. T2-K^{b} APCs expressing H-$2K^{b}$ were preloaded with either the null peptide (pFARL), the antigenic peptide (pOVA), or no peptide and cocultured with OT-I $Rag^{-/-}$ $\beta2m^{-/-}$ thymocytes in the presence or absence of anti-CD3. Subsequent CD3-PD assay showed that both cognate pOVA and Ab stimulation induced open-CD3 above basal levels in the cocultures (Fig. 5*A*, *bottom panel*). We observed that the open-CD3 induced by soluble anti-CD3 stimulation coprecipitated the stimulatory Ab itself, indicating that ligand engagement remained intact throughout the pull-down procedure (Fig. 5*A*, *top panel*). However, there was no coprecipitation of H-$2K^{b}$ H chain associated with the open-CD3 induced by pOVA (Fig. 5*A*, *middle panel*), indicating that open-CD3 outlived ligand dissociation. Because the previously cited work that defined an instantaneously reversible open-CD3 used the T1 TCR system (26), we sought to determine whether our result above was attributable to the use of a different TCR system. The T1 TCR is restricted to a chemically modified peptide derived from *Plasmodium berghei* (pSYIP) presented by H-$2K^{d}$. P-815 APCs expressing H-$2K^{d}$ were preloaded with either no peptide or the cognate pSIYP and cocultured with T1 hybridoma cells in the presence or absence of anti-CD3. In this experiment, an immunoprecipitation of the H2-K^{d} molecule from pSIYP-stimulated samples was included to examine whether the pSIYP/H2-K^{d}:TCR–CD3 engaged interaction could survive cell

NIH-PA Author Manuscript

NIH-PA Author Manuscript

NIH-PA Author Manuscript

lysis and pull-down. Probably due to the low affinity of pMHC:TCR interaction, no detectable coprecipitation of CD3 with H2-K^d was observable by WB (Fig. 5*B*). Still, the resulting CD3-PD assay showed similar results to those obtained in the OT-I system. Ab stimulation induced open-CD3 above basal levels (Fig. 5*B*, *bottom panel*), and the stimulatory Ab coprecipitated with open-CD3 (Fig. 5*B*, *top panel*). In contrast, the pSIYP stimulation induced open-CD3 as well (Fig. 5*B*, *bottom panel*), but there was no coprecipitation of H-$2K^d$ with the pSIYP-stimulated open-CD3 (Fig. 5*B*, *middle panel*). Taken together, these data provide an example of a high-affinity ligand (anti-CD3) that does not dissociate from CD3 and a low-affinity ligand (pSIYP/H2-K^d) that does dissociate, yet in both cases we detect induced open-CD3. Therefore, we conclude that when pMHC from APC engages TCR, the open-CD3 conformation is induced such that it remains intact subsequent to the dissociation of the engaging ligand and does not revert instantaneously to the closed-CD3 conformation.

The CD3ε BRS is not required to conceal the PRS in absence of TCR–CD3 engagement

We wished to examine whether the ability of the CD3ε BRS motif to interact with phosphoinositides could influence PRS accessibility to Nck. To do so, we compared thymocytes from B6 mice transgenic for either CD3ε BRS WT or BRS-Substitute (19), where the substituted amino acids replace the basic residues and abrogate lipid association (Fig. 6*A*). Thymocytes were treated in vitro with APA1/1, Ham IgG, or anti-CD3 mAb 2C11 prior to the CD3-PD assay to calculate background, basal, and stimulated open-CD3 levels. In six independent experiments, we found that basal open-CD3 levels were similar in both mice (average % Max. of Stimulation: BRS WT = 37%, BRS-Substitute = 39%; Fig. 6*B*, 6*C*). Moreover, anti-CD3 stimulation induced open-CD3 above basal levels equivalently (average Open-CD3: BRS WT = 2.8, BRS-Substitute = 3.2; Fig. 6*B*, 6*D*). These data indicate that the phosphoinositide binding capacity of the BRS is not required either for adoption of the closed-CD3 conformation or for induction of open-CD3 by Ab stimulation.

Discussion

Although the PRS of CD3ε is considered to be of structural and functional importance, there are currently two opposing ideas that have been published regarding the regulation of its accessibility to Nck-SH3.1 binding: i) the PRS is constitutively exposed (12, 14); and ii) the PRS is inducibly exposed via CD3Δc upon TCR–CD3 engagement (5–7). In performing experiments designed to reconcile these two scenarios, we have determined that both constitutive and inducible PRS exposure occur, but each at a distinct level. First, our data confirms that primary thymocytes express a positive basal level of mature αβ TCR–CD3 complexes in the open-CD3 conformation, even in the absence of TCR engagement. Second, Ag presentation in vivo is capable of inducing open-CD3 and contributing to basal levels in thymocytes from MHC^+ mice. Third, exogenous TCR–CD3 engagement significantly increases the number of complexes adopting open-CD3 beyond the basal level, consistent with previous work that focused on this induction as an outcome of CD3Δc.

To arrive at these conclusions, we first revisited the question of whether TCR–CD3 engagement promotes the exposure of the PRS in murine thymocytes. After performing statistical analysis of data generated by the CD3-PD assay in 22 independent tests, we established a mean induction of open-CD3 stimulated by anti-CD3 treatment of 4.4-fold the level of open-CD3 found in nonstimulated thymocytes (Fig. 1*C*). Thus, we propose that TCR–CD3 engagement consistently induces CD3Δc in thymocytes, increasing the amount of Nck-accessible PRS upon stimulation. It is likely that the low inducibility reported elsewhere by the CD3-PD assay [1.2- to 1.5-fold (12); 1.4- to 1.6-fold (14)] falls within the low but positive natural variance, consistent with the statistical analysis reported in this study. However, using an alternative method to the CD3-PD assay for detecting open-CD3

NIH-PA Author Manuscript

NIH-PA Author Manuscript

NIH-PA Author Manuscript

(7, 8, 11), one group showed that the CD3ε of thymocytes was accessible to the mAb APA1/1 irrespective of stimulation (12), suggesting again a constitutive exposure of the PRS [as this motif partially overlaps with the epitope for the mAb (29)]. We replicated their observation using APA1/1 staining as a readout (Fig. 4); however, by performing the CD3-PD assay in parallel (Fig. 3), we found that the CD3-PD assay was sensitive to TCR–CD3 engagement in experiments where APA1/1 binding was fully positive regardless of engagement (Fig. 4*A*–*C*). These results indicate that APA1/1 staining and the CD3-PD assay assess two different properties of CD3ε protein expression and cannot be used interchangeably by the methods described in this study. In our experiments, APA1/1 bound CD3ε independently of TCR–CD3 engagement (Fig. 4). Therefore, APA1/1 revealed total CD3ε protein expression, regardless of stimulation. In contrast, the results of the CD3-PD assay performed in parallel were dependent on TCR–CD3 engagement (Fig. 3). Therefore, CD3-PD assay assessed the level of open-CD3 but not total CD3ε protein expression. We conclude that TCR–CD3 engagement increases the level of PRS accessibility to Nck and is best observed using an assay that employs the $SH3.1_{Nck}$ domain itself.

To confirm the specificity of basal open-CD3, we compared the level found in nonstimulated thymocytes with the background of the CD3-PD assay. As an average, levels of open-CD3 in nonstimulated thymocytes were 5.3-fold higher than the background, whereas levels in stimulated thymocytes reached 20.8-fold (Fig. 2*C*). Thus, we observed basal open-CD3 in nonstimulated thymocytes and distinguished it from the nonspecific background of the CD3-PD assay (Fig. 2). Because we had previously shown that weak antigenic engagement induces open-CD3 in preselection DP OT-I thymocytes (6), we hypothesized that Ags mediating selection in the B6 thymus might cause to some degree basal open-CD3 in thymocytes. To test this possibility, we compared the basal open-CD3 found in thymocytes isolated from B6 WT and $Abb^{-/-}$ $\beta2m^{-/-}$ mice, the latter lacking Ag presentation due to deficiencies in MHC expression. Basal open-CD3 found in B6 $Abb^{-/-}$ $\beta2m^{-/-}$ mice was lower than in B6 WT (Fig. 3*A*, 3*B*). These data suggest that Ags presented in the thymus are able to induce open-CD3 in a WT TCR repertoire in vivo. However, nonstimulated $Abb^{-/-}$ $\beta2m^{-/-}$ thymocytes still contained half the amount of open-CD3 found in B6 WT thymocytes (Fig. 3*A*, 3*B*). Therefore, some basal open-CD3 occurs in the absence of TCR:pMHC engagement by conventional MHC-based ligands. Basal open-CD3 could sustain the ligand-independent regulation of TCR–CD3 surface expression level in DP thymocytes proposed in previous reports (12, 13, 16). In addition, different thymocyte subsets may possibly exhibit distinct levels of open-CD3 that could contribute to the basal levels we measure from the bulk thymocyte population. For example, some γδ thymocytes not restricted to MHC-related molecules might still interact with ligands in the thymus of $Abb^{-/-}$ $\beta2m^{-/-}$ mice and contribute to basal open-CD3. Alternatively, the pre-TCR expressed by double-negative thymocytes has been shown to signal in the absence of engagement by extrinsic ligands (34) and to display open-CD3 in the absence of anti-CD3 stimulation (14). Future experimentation will be required to characterize further basal open-CD3 and determine its functional impact in diverse thymocyte populations.

A recent study showed that open-CD3 could be induced by soluble pMHC class I tetramers, but the conformation reverted to closed-CD3 as soon as the TCR lost contact with the ligand (9). In those experiments, positive capture of open-CD3 also coprecipitated the engaging ligand MHC class I (MHC-I), as assessed by the CD3-PD assay. However, we did not find specific MHC-I coprecipitation with open-CD3 induced by Ag-loaded APCs in either of two class I-restricted TCRs tested (Fig. 5). Thus, we propose that TCR engagement by class I Ags associated with APCs imposes some distinct property that stabilizes open-CD3 to outlast TCR ligand dissociation (Fig. 7). According to mathematical models applied to evaluate the role of serial engagement and kinetic proofreading in the process of TCR–CD3 internalization, the receptors must remain tagged for endocytosis after dissociation from Ags

NIH-PA Author Manuscript

NIH-PA Author Manuscript

NIH-PA Author Manuscript

(35). Given that the PRS has been related to TCR–CD3 endocytosis, ubiquitylation, and degradation (12, 14, 16, 36), an interesting possibility emerges that open-CD3 might mark post-engaged receptors and link them in some way to endocytosis and/or recycling processes.

Through its cytosolic BRS motif, the CD3ε tail has been proposed to interact with specific phosphoinositides at the inner leaflet of the plasma membrane (18, 19). This interaction can sustain a partial folding of the distal ITAM, embedding the tyrosine residues into the hydrophobic core of the lipid bilayer (18). The possibility was suggested that the lipid-bound BRS might cause the PRS to adopt its closed conformation, preventing its access to cytosolic binding partners (23). However, a subsequent study of naive T cells containing CD3ε molecules unable to complex lipids revealed only small differences in signaling pathways in response to anti-CD3 and pMHC stimulations while suggesting a more prominent role of the BRS in the regulation of TCR–CD3 recycling (19). To test whether the BRS was required to conceal the PRS, we compared the contents of open-CD3 in mice transgenic for CD3ε BRS WT and CD3ε BRS-Substitute sequences, the latter lacking BRS–lipid binding capability (19).We found that regarding both basal open-CD3 (Fig. 6*C*) and Ab-inducible open-CD3 (Fig. 6*D*), BRS-Substitute thymocytes were equal to their BRS WT counterparts. Thus, the BRS does not appear to be required to cause PRS concealment in closed-CD3 or to promote PRS exposure upon Ab stimulation.

In summary, in this study we present an updated model of the regulation of PRS accessibility in thymocytes that unifies previous observations regarding the constitutive versus inducible nature of PRS accessibility to Nck. First, we observe a basal level of open-CD3 in thymocytes that is compatible with Ag-independent PRS participation in the regulation of TCR–CD3 expression. Second, we demonstrate that antigenic engagement in thymocytes elevates open-CD3 above basal levels, consistent with the idea that thymocytes undergo CD3Δc upon stimulation. We also show that Ags expressed by APCs can induce open-CD3 that outlasts ligand dissociation from the TCR. Finally, the BRS motif in CD3ε is required for neither concealment nor exposure of the PRS. Future experimentation will explore in greater detail the factors that influence basal open-CD3 and the duration and function of CD3 conformations in T cells of various maturation states.

Acknowledgments

We thank Chella David, Raif Geha, Ed Palmer, Hidde L. Ploegh, and Terry Potter for providing reagents; Dan Billadeau, Mark Daniels, Tim Gomez, Karen Hedin, Larry Pease, Jim Tarara, and Emma Teixeiro for helpful discussion; and Robert Stiles and Tessa Davis for excellent technical assistance.

This work was supported by base-budget funds from the Mayo Foundation (to D.G. and A.G.S.), Grant PI060057 from the Instituto de Salud Carlos III (to D.G.), Training Grant R25 GM 75148 from the National Institutes of Health (to the College of Medicine, Mayo Clinic, for J.d.l.C.), the Mayo Clinic Summer Undergraduate Research Fellowship program (to T.K. and C.A.P.), National Institutes of Health Grants AI42953 and AI71229 (to N.S.C.v.O.), and Grant 310030-125330 from the Swiss National Foundation (to I.F.L.).

Abbreviations used in this article

ABA	4-azidobenzoic acid
AF	Alexa Fluor
B6	C57BL/6
BRS	basic amino acid-rich stretch
CD3Δc	CD3 conformational change

NIH-PA Author Manuscript

NIH-PA Author Manuscript

NIH-PA Author Manuscript

CD3-PD	CD3 pull-down
DP	double-positive
Ham IgG	hamster IgG isotype control
MHC-I	MHC class I
pMHC	peptide–MHC
PRS	proline-rich sequence
TL	total lysate
WB	Western blot
WT	wild-type

References

1. Reth M. Antigen receptor tail clue. Nature. 1989; 338:383–384. [PubMed: 2927501]
2. Smith-Garvin JE, Koretzky GA, Jordan MS. T cell activation. Annu. Rev. Immunol. 2009; 27:591–619. [PubMed: 19132916]
3. Cohn M. Tritope model of restrictive recognition by the TCR. Trends Immunol. 2003; 24:127–131. [PubMed: 12615207]
4. Janeway CA Jr. Ligands for the T-cell receptor: hard times for avidity models. Immunol. Today. 1995; 16:223–225. [PubMed: 7779252]
5. Gil D, Schamel WW, Montoya M, Sánchez-Madrid F, Alarcón B. Recruitment of Nck by CD3 epsilon reveals a ligand-induced conformational change essential for T cell receptor signaling and synapse formation. Cell. 2002; 109:901–912. [PubMed: 12110186]
6. Gil D, Schrum AG, Alarcón B, Palmer E. T cell receptor engagement by peptide-MHC ligands induces a conformational change in the CD3 complex of thymocytes. J. Exp. Med. 2005; 201:517–522. [PubMed: 15728235]
7. Risueño RM, Gil D, Fernández E, Sánchez-Madrid F, Alarcón B. Ligand-induced conformational change in the T-cell receptor associated with productive immune synapses. Blood. 2005; 106:601–608. [PubMed: 15790785]
8. Risueño RM, van Santen HM, Alarcón B. A conformational change senses the strength of T cell receptor-ligand interaction during thymic selection. Proc. Natl. Acad. Sci. USA. 2006; 103:9625–9630. [PubMed: 16766661]
9. Minguet S, Swamy M, Alarcón B, Luescher IF, Schamel WW. Full activation of the T cell receptor requires both clustering and conformational changes at CD3. Immunity. 2007; 26:43–54. [PubMed: 17188005]
10. Szymczak AL, Workman CJ, Gil D, Dilioglou S, Vignali KM, Palmer E, Vignali DA. The CD3epsilon proline-rich sequence, and its interaction with Nck, is not required for T cell development and function. J. Immunol. 2005; 175:270–275. [PubMed: 15972658]
11. Tailor P, Tsai S, Shameli A, Serra P, Wang J, Robbins S, Nagata M, Szymczak-Workman AL, Vignali DA, Santamaria P. The proline-rich sequence of CD3epsilon as an amplifier of low-avidity TCR signaling. J. Immunol. 2008; 181:243–255. [PubMed: 18566390]
12. Mingueneau M, Sansoni A, Grégoire C, Roncagalli R, Aguado E, Weiss A, Malissen M, Malissen B. The proline-rich sequence of CD3epsilon controls T cell antigen receptor expression on and signaling potency in pre-selection CD4+CD8+ thymocytes. Nat. Immunol. 2008; 9:522–532. [PubMed: 18408722]
13. Brodeur JF, Li S, Damlaj O, Dave VP. Expression of fully assembled TCR-CD3 complex on double positive thymocytes: synergistic role for the PRS and ER retention motifs in the intra-cytoplasmic tail of CD3epsilon. Int. Immunol. 2009; 21:1317–1327. [PubMed: 19819936]

NIH-PA Author Manuscript

NIH-PA Author Manuscript

NIH-PA Author Manuscript

14. Brodeur JF, Li S, Martins Mda. S, Larose L, Dave VP. Critical and multiple roles for the CD3epsilon intracytoplasmic tail in double negative to double positive thymocyte differentiation. J. Immunol. 2009; 182:4844–4853. [PubMed: 19342663]
15. Dave VP. Hierarchical role of CD3 chains in thymocyte development. Immunol. Rev. 2009; 232:22–33. [PubMed: 19909353]
16. Wang H, Holst J, Woo SR, Guy C, Bettini M, Wang Y, Shafer A, Naramura M, Mingueneau M, Dragone LL, et al. Tonic ubiquitylation controls T-cell receptor:CD3 complex expression during T-cell development. EMBO J. 2010; 29:1285–1298. [PubMed: 20150895]
17. Maltzman JS, Koretzky GA. CD3varepsilon: PeRuSing for positive selection. Nat. Immunol. 2008; 9:457–459. [PubMed: 18425097]
18. Xu C, Gagnon E, Call ME, Schnell JR, Schwieters CD, Carman CV, Chou JJ, Wucherpfennig KW. Regulation of T cell receptor activation by dynamic membrane binding of the CD3epsilon cytoplasmic tyrosine-based motif. Cell. 2008; 135:702–713. [PubMed: 19013279]
19. Deford-Watts LM, Tassin TC, Becker AM, Medeiros JJ, Albanesi JP, Love PE, Wülfing C, van Oers NS. The cytoplasmic tail of the T cell receptor CD3 epsilon subunit contains a phospholipid-binding motif that regulates T cell functions. J. Immunol. 2009; 183:1055–1064. [PubMed: 19542373]
20. Sigalov AB, Aivazian DA, Uversky VN, Stern LJ. Lipid-binding activity of intrinsically unstructured cytoplasmic domains of multichain immune recognition receptor signaling subunits. Biochemistry. 2006; 45:15731–15739. [PubMed: 17176095]
21. Aivazian D, Stern LJ. Phosphorylation of T cell receptor zeta is regulated by a lipid dependent folding transition. Nat. Struct. Biol. 2000; 7:1023–1026. [PubMed: 11062556]
22. Dustin ML. The cellular context of T cell signaling. Immunity. 2009; 30:482–492. [PubMed: 19371714]
23. Kuhns MS, Davis MM. The safety on the TCR trigger. Cell. 2008; 135:594–596. [PubMed: 19013269]
24. DeJarnette JB, Sommers CL, Huang K, Woodside KJ, Emmons R, Katz K, Shores EW, Love PE. Specific requirement for CD3epsilon in T cell development. Proc. Natl. Acad. Sci. USA. 1998; 95:14909–14914. [PubMed: 9843989]
25. Luescher IF, Anjuère F, Peitsch MC, Jongeneel CV, Cerottini JC, Romero P. Structural analysis of TCR-ligand interactions studied on H-2Kd-restricted cloned CTL specific for a photoreactive peptide derivative. Immunity. 1995; 3:51–63. [PubMed: 7621078]
26. Luescher IF, Cerottini JC, Romero P. Photoaffinity labeling of the T cell receptor on cloned cytotoxic T lymphocytes by covalent photoreactive ligand. J. Biol. Chem. 1994; 269:5574–5582. [PubMed: 8119892]
27. Potter TA, Rajan TV, Dick RF II, Bluestone JA. Substitution at residue 227 of H-2 class I molecules abrogates recognition by CD8-dependent, but not CD8-independent, cytotoxic T lymphocytes. Nature. 1989; 337:73–75. [PubMed: 2462676]
28. Schrum AG, Gil D, Dopfer EP, Wiest DL, Turka LA, Schamel WW, Palmer E. High-sensitivity detection and quantitative analysis of native protein-protein interactions and multiprotein complexes by flow cytometry. Sci. STKE. 2007; 2007:pl2. [PubMed: 17551170]
29. Alarcón B, Ley SC, Sánchez-Madrid F, Blumberg RS, Ju ST, Fresno M, Terhorst C. The CD3-gamma and CD3-delta subunits of the T cell antigen receptor can be expressed within distinct functional TCR/CD3 complexes. EMBO J. 1991; 10:903–912. [PubMed: 1826255]
30. Grusby MJ, Auchincloss H Jr, Lee R, Johnson RS, Spencer JP, Zijlstra M, Jaenisch R, Papaioannou VE, Glimcher LH. Mice lacking major histocompatibility complex class I and class II molecules. Proc. Natl. Acad. Sci. USA. 1993; 90:3913–3917. [PubMed: 8483910]
31. Hogquist KA, Jameson SC, Heath WR, Howard JL, Bevan MJ, Carbone FR. T cell receptor antagonist peptides induce positive selection. Cell. 1994; 76:17–27. [PubMed: 8287475]
32. Harder T, Simons K. Caveolae, DIGs, and the dynamics of sphingolipid-cholesterol microdomains. Curr. Opin. Cell Biol. 1997; 9:534–542. [PubMed: 9261060]
33. Gil D, Schrum AG, Daniels MA, Palmer E. A role for CD8 in the developmental tuning of antigen recognition and CD3 conformational change. J. Immunol. 2008; 180:3900–3999. [PubMed: 18322198]

NIH-PA Author Manuscript

NIH-PA Author Manuscript

NIH-PA Author Manuscript

34. Yamasaki S, Ishikawa E, Sakuma M, Ogata K, Sakata-Sogawa K, Hiroshima M, Wiest DL, Tokunaga M, Saito T. Mechanistic basis of pre-T cell receptor-mediated autonomous signaling critical for thymocyte development. Nat. Immunol. 2006; 7:67–75. [PubMed: 16327787]

35. Coombs D, Kalergis AM, Nathenson SG, Wofsy C, Goldstein B. Activated TCRs remain marked for internalization after dissociation from pMHC. Nat. Immunol. 2002; 3:926–931. [PubMed: 12244312]

36. Takeuchi K, Yang H, Ng E, Park SY, Sun ZY, Reinherz EL, Wagner G. Structural and functional evidence that Nck interaction with CD3epsilon regulates T-cell receptor activity. J. Mol. Biol. 2008; 380:704–716. [PubMed: 18555270]

NIH-PA Author Manuscript
NIH-PA Author Manuscript
NIH-PA Author Manuscript

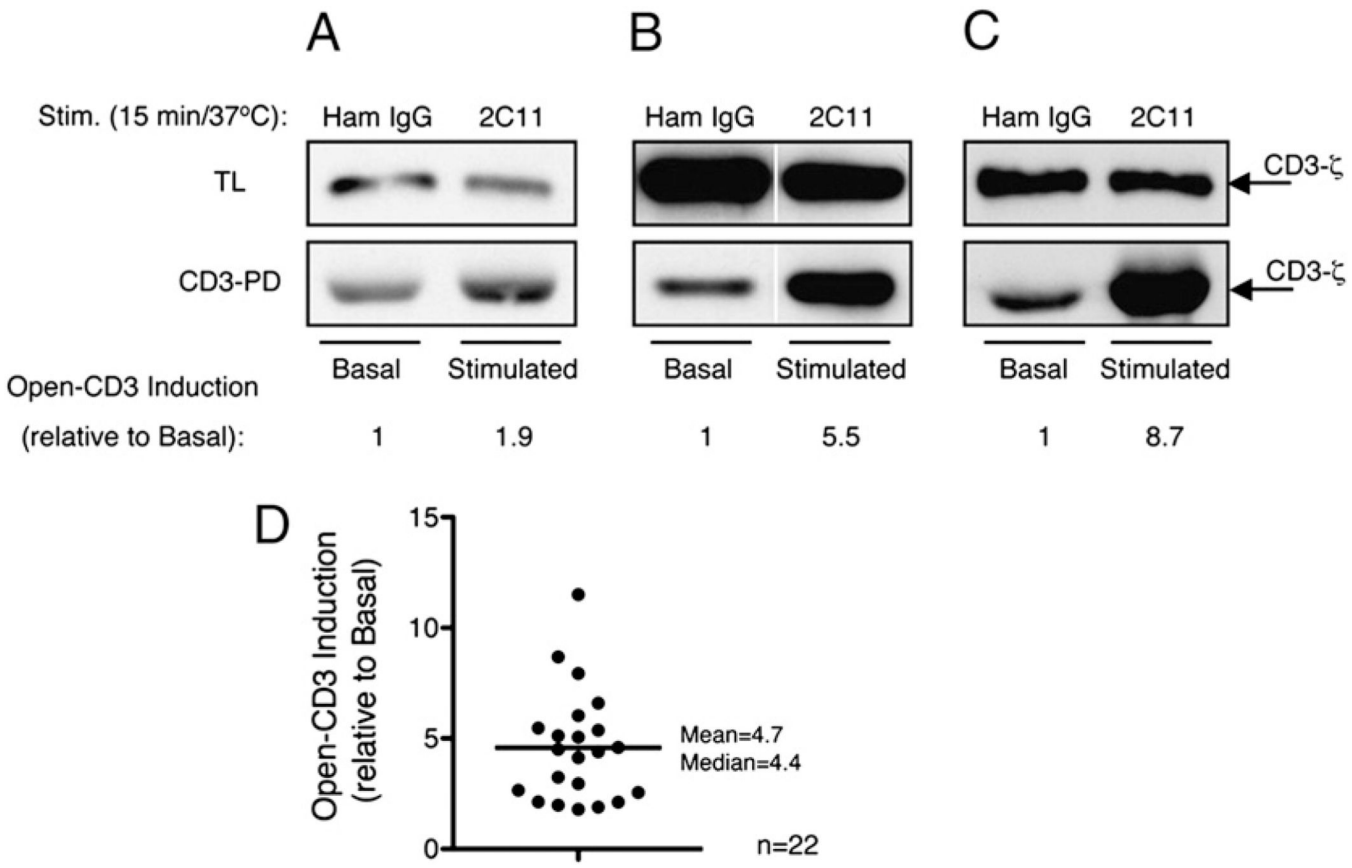

FIGURE 1.

TCR–CD3 engagement induces open-CD3 in B6 thymocytes. B6 thymocytes were treated in vitro with either Ham IgG (basal condition) or anti-CD3ε mAb 2C11 (stimulated condition). Next, cells were lysed and either total lysate (TL) or CD3-PD assay samples were prepared (see *Materials and Methods*), involving SDS-PAGE and WB for CD3ζ. Twenty-two independent CD3-PD assays were performed, and open-CD3 induction was calculated in each as the ratio of open-CD3 found in stimulated relative to basal conditions. *A–C*, Three independent experiments are shown representing low (*A*), intermediate (*B*), and high (*C*) levels of induced open-CD3 by 2C11 stimulation. *D*, Values of open-CD3 induction achieved by 2C11 stimulation are plotted (mean = 4.7, median = 4.4, SD = 2.6, SE = 0.5).

NIH-PA Author Manuscript
NIH-PA Author Manuscript
NIH-PA Author Manuscript

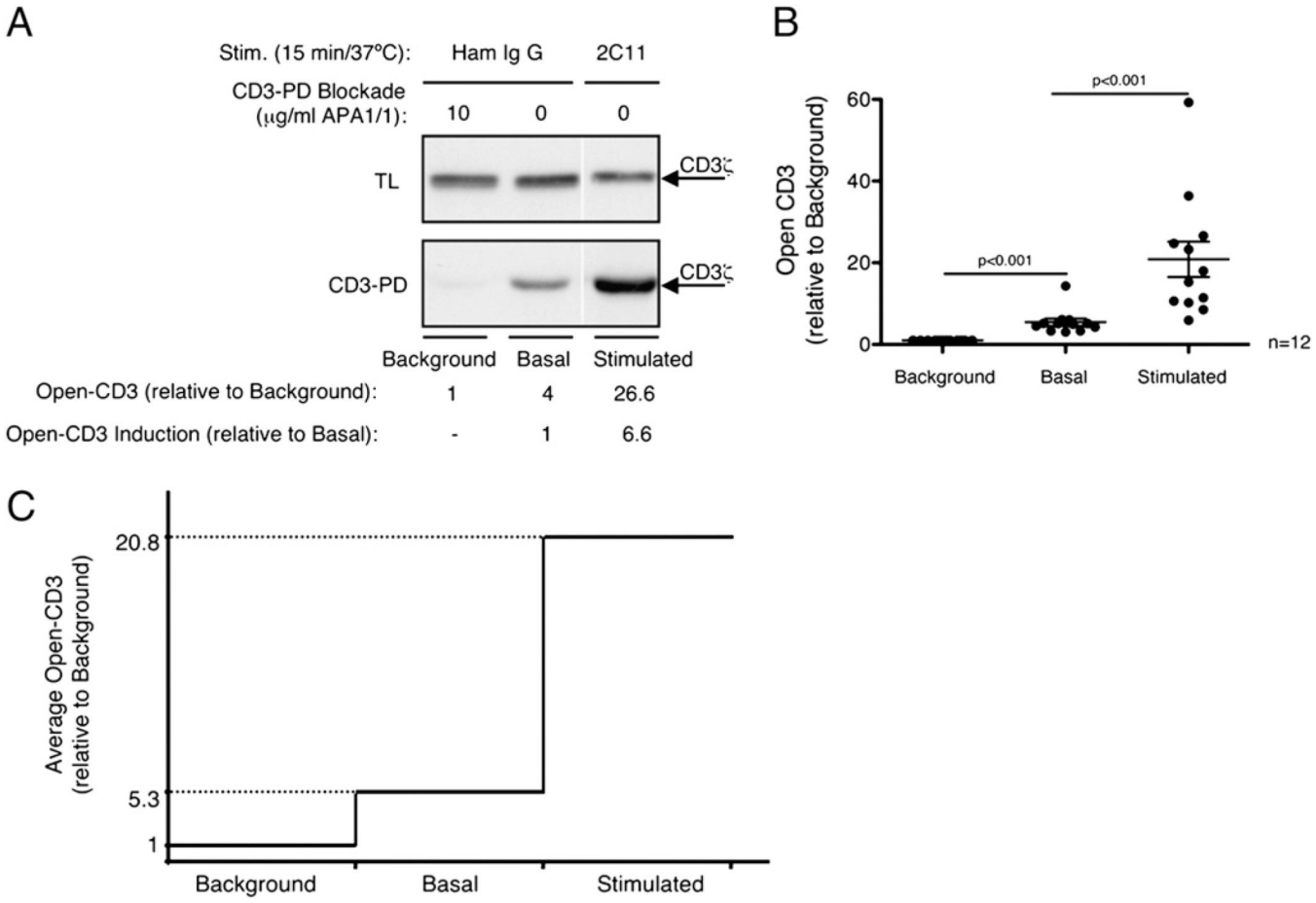

FIGURE 2.

Nonstimulated B6 thymocytes express basal levels of open-CD3. B6 thymocytes were treated in vitro with either Ham IgG (basal condition) or anti-CD3ε mAb 2C11 (stimulated condition). Then samples were subjected to the CD3-PD assay either in the presence or the absence of the blocking mAb APA1/1 to compare the assay background with specific basal and stimulated open-CD3. *A*, One representative experiment illustrating the amount of open-CD3 in background, basal, and 2C11-stimulated conditions. The fold-increases are shown relative to either background or basal open-CD3. *B*, Values of open-CD3 found in basal and stimulated conditions are plotted relative to the CD3-PD assay background in 12 independent experiments. Lines represent the mean open-CD3 found in each condition; SE bars for each condition are shown. Paired *t* tests were run to calculate *p* values; basal open-CD3 is statistically different from background, and stimulated open-CD3 is statistically different from basal. *C*, Mean of basal and stimulated amounts of open-CD3 established in these 12 independent experiments relative to CD3-PD assay background are depicted.

NIH-PA Author Manuscript
NIH-PA Author Manuscript
NIH-PA Author Manuscript

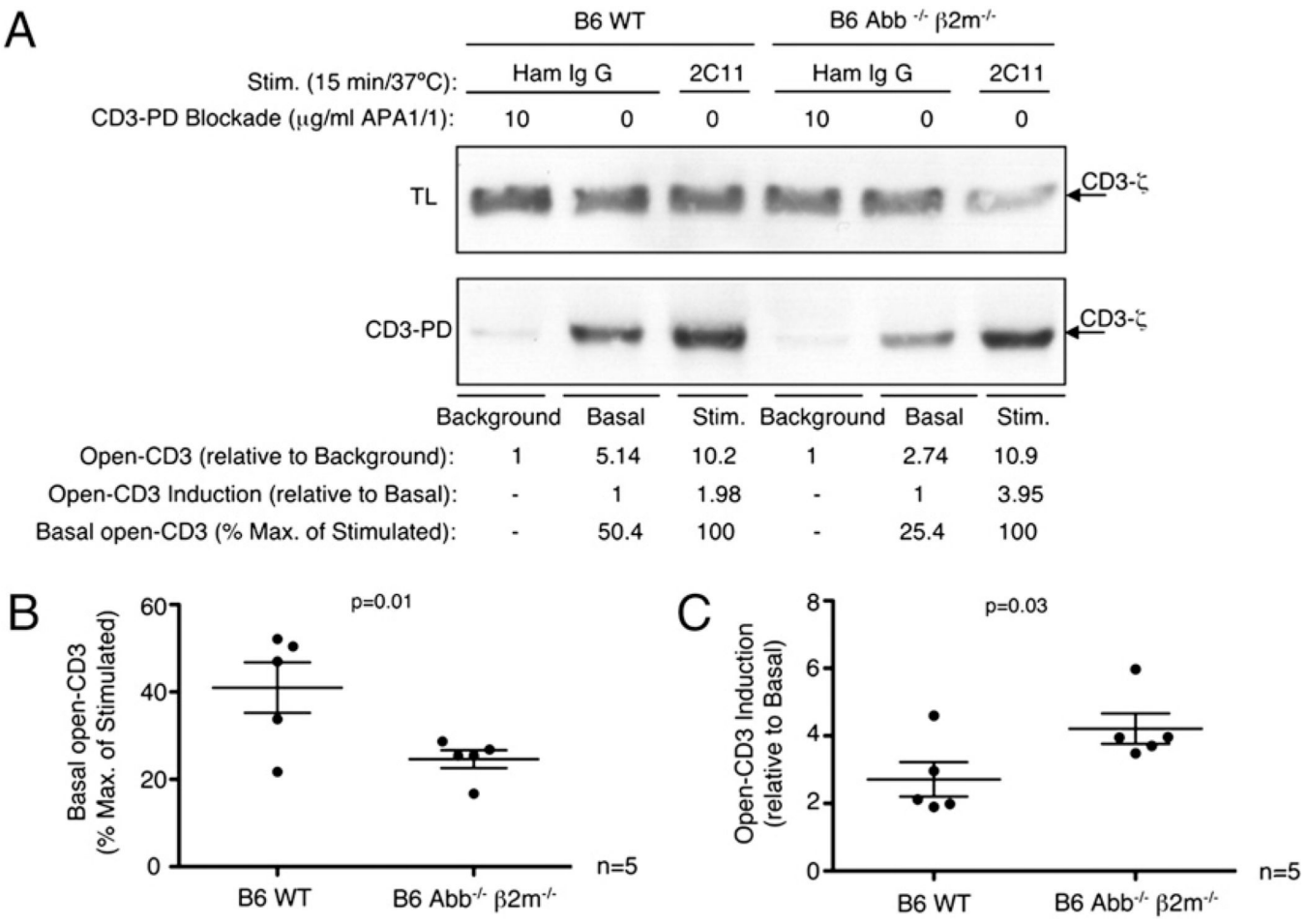

FIGURE 3.

Thymic MHC induces basal open-CD3 in WT thymocytes in vivo. Background, basal, and stimulated samples were prepared from B6 WT or B6 Abb$^{-/-}$ β2m$^{-/-}$ thymocytes to establish the amounts of open-CD3 using the CD3-PD assay. Amounts of open-CD3 relative to either the CD3-PD assay background or basal conditions were calculated for both types of thymocytes as in Fig. 2. Additionally, percent maximum (2C11 stimulation = 100%) was calculated to facilitate the comparison of basal open-CD3 observed from each thymocyte type. *A*, The measurements of open-CD3 found in B6 WT and Abb$^{-/-}$ β2m$^{-/-}$ mice from one representative experiment are shown. *B* and *C*, Values of basal open-CD3 as a percent maximum of 2C11 stimulation (*B*) and open-CD3 induction achieved by 2C11stimulation over basal (*C*) are plotted for five independent experiments. The mean ± SE is displayed representing the amount of open-CD3 found in thymocytes from each mouse type. Paired *t* tests were run to calculate *p* values.

NIH-PA Author Manuscript
NIH-PA Author Manuscript
NIH-PA Author Manuscript

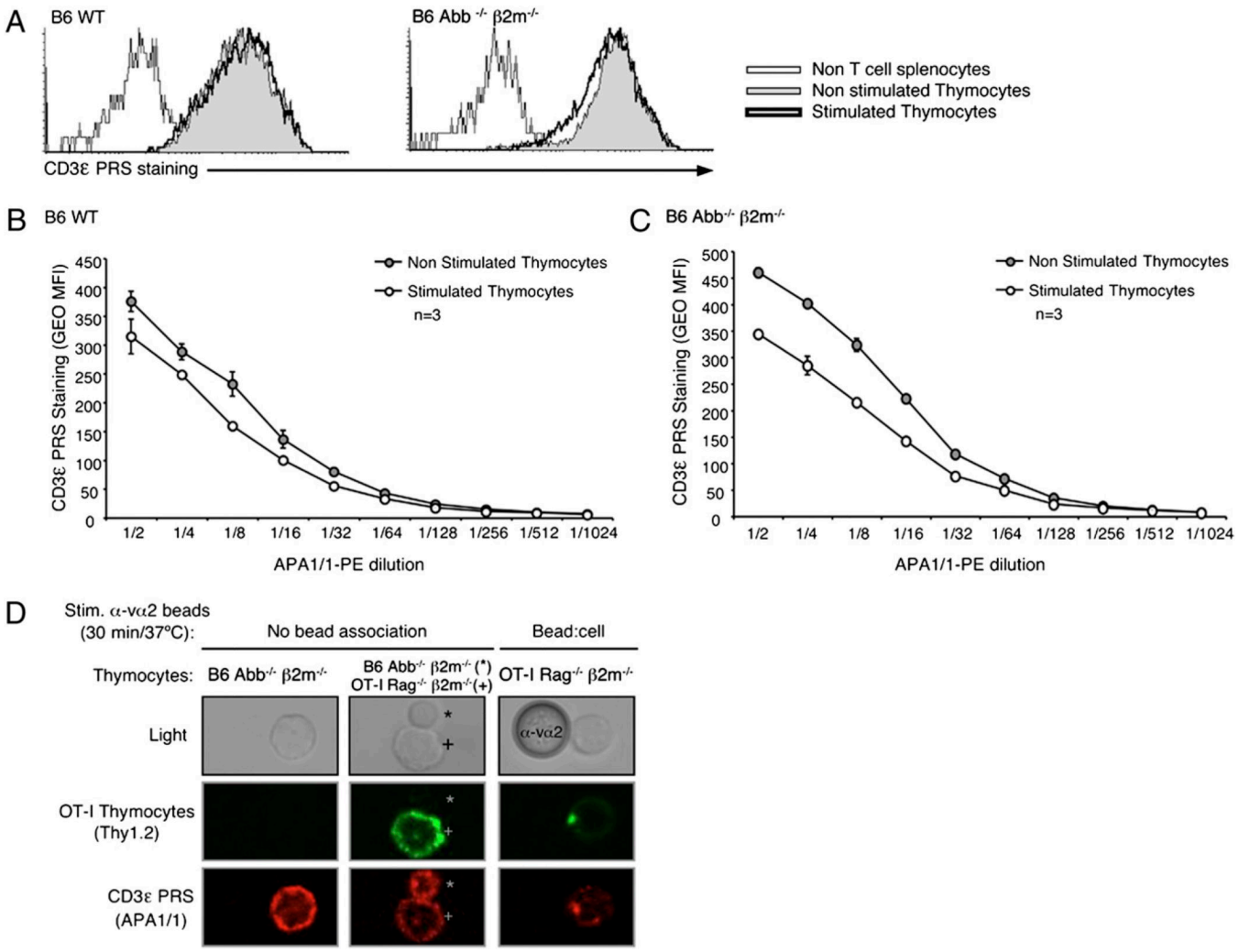

FIGURE 4.

The mAb APA1/1 can bind to the CD3ε cytoplasmic tail independently of TCR–CD3 engagement. Flow cytometry via intracellular staining of the CD3ε PRS using the mAb APA1/1 was performed in parallel to the CD3-PD assay in all nonstimulated and stimulated samples shown in Fig. 3. Splenocytes from B6 Abb$^{-/-}$ β2m$^{-/-}$ mice were added to the samples right after the stimulation, and before the fixation/permeabilization protocol, to provide a non-T cell population and establish the background of this staining. *A*, Data are from the same experiment shown in Fig. 3*A*. Histograms are displayed overlaying the CD3ε PRS staining (with 1:2 dilution of APA1/1–PE) of thymocytes treated with either Ham IgG (basal condition) or anti-CD3 mAb 2C11 (stimulated condition) for 15 min at 37°C. *B* and *C*, CD3ε PRS stain in B6 WT (*B*) or Abb$^{-/-}$ β2m$^{-/-}$ (*C*) thymocytes with decreasing doses of APA1/1–PE is displayed for data from the same experiment shown in Fig. 3*A*. *D*, OT-I Rag2$^{-/-}$ β2m$^{-/-}$ thymocytes were labeled in the cold with anti-Thy1.2-biotin plus streptavidin–AF-488, mixed with anti-Vα2 polystyrene latex beads (1:4 ratio), stimulated 30 min at 37°C, and treated with Cytofix/Cytoperm buffer. Samples were then mixed with B6 Abb$^{-/-}$ β2m$^{-/-}$ nonstimulated thymocytes that had been fixed and permeabilized in parallel. The resulting samples were then stained intracellularly with APA1/1–AF-555 and mounted on coverslips for confocal analysis. Micrographs display images at ~×60 magnification, and the anti-Va2 bead is 5 μm in diameter.

NIH-PA Author Manuscript
NIH-PA Author Manuscript
NIH-PA Author Manuscript

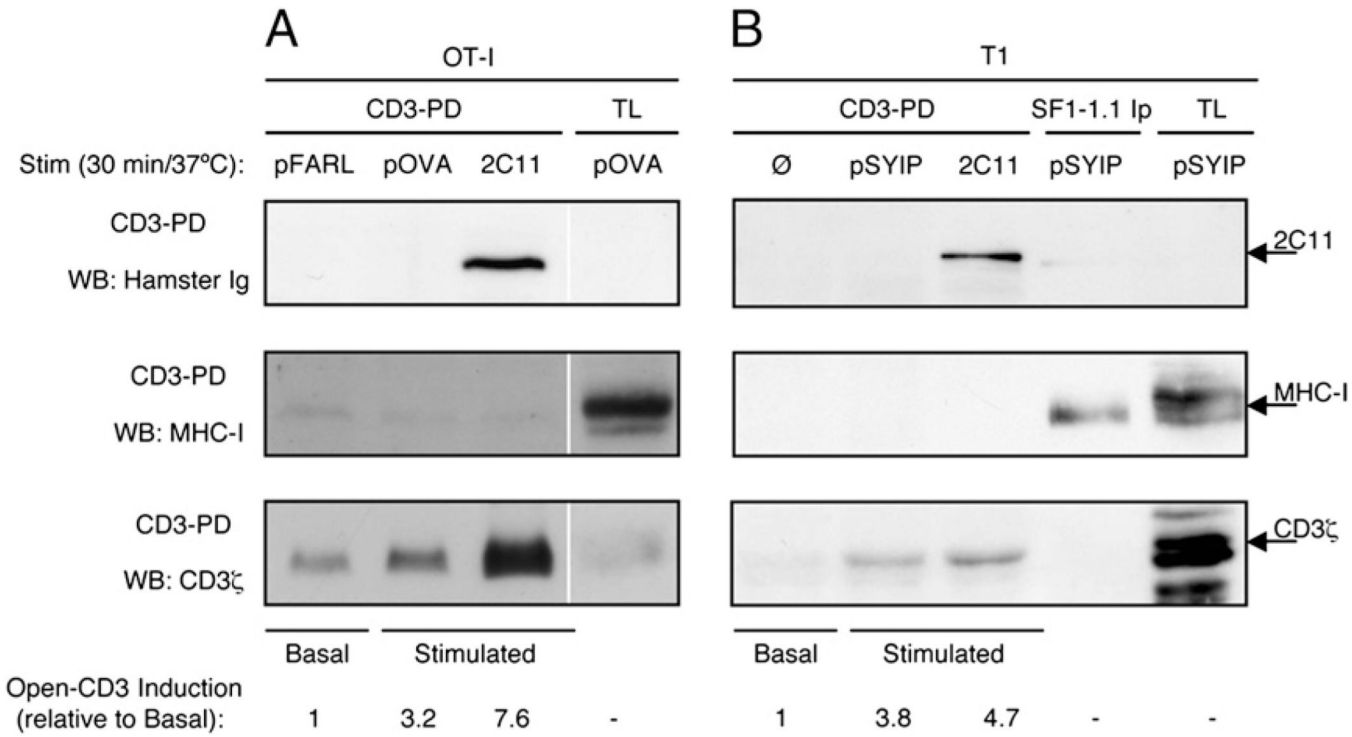

FIGURE 5.

Open-CD3 outlasts TCR engagement by APCs. *A*, OT-I Rag$^{-/-}$ β2m$^{-/-}$ preselection DP thymocytes were cocultured for 30 min at 37°C with T2-K^{b} APCs that had been preloaded with either pFARL (null peptide), pOVA (antigenic peptide), or no peptide plus soluble anti-CD3ε mAb 2C11. Then, cocultures were lysed and subjected to the CD3-PD assay. CD3-PD samples were visualized for their content of 2C11, MHC-I H chain, and CD3ζ by WB. Open-CD3 inductions achieved by antigenic and 2C11 stimulation were calculated relative to the amounts of open-CD3 found in basal conditions (pFARL). *B*, T1 hybridoma cells were cocultured for 30 min with P-815 APCs that had been preloaded with either no peptide (Ø), pSYIP (antigenic peptide), or no peptide plus soluble anti-CD3ε mAb 2C11. Then, cocultures were lysed and subjected to the CD3-PD assay or H2-K^{d} immunoprecipitation with the mAb SF1-1.1. CD3-PD samples were visualized for their content of 2C11, MHC-I H chain, and CD3ζ by WB. Open-CD3 inductions achieved by antigenic and 2C11 stimulation were calculated relative to the amounts of open-CD3 found in basal conditions (Ø).

NIH-PA Author Manuscript
NIH-PA Author Manuscript
NIH-PA Author Manuscript

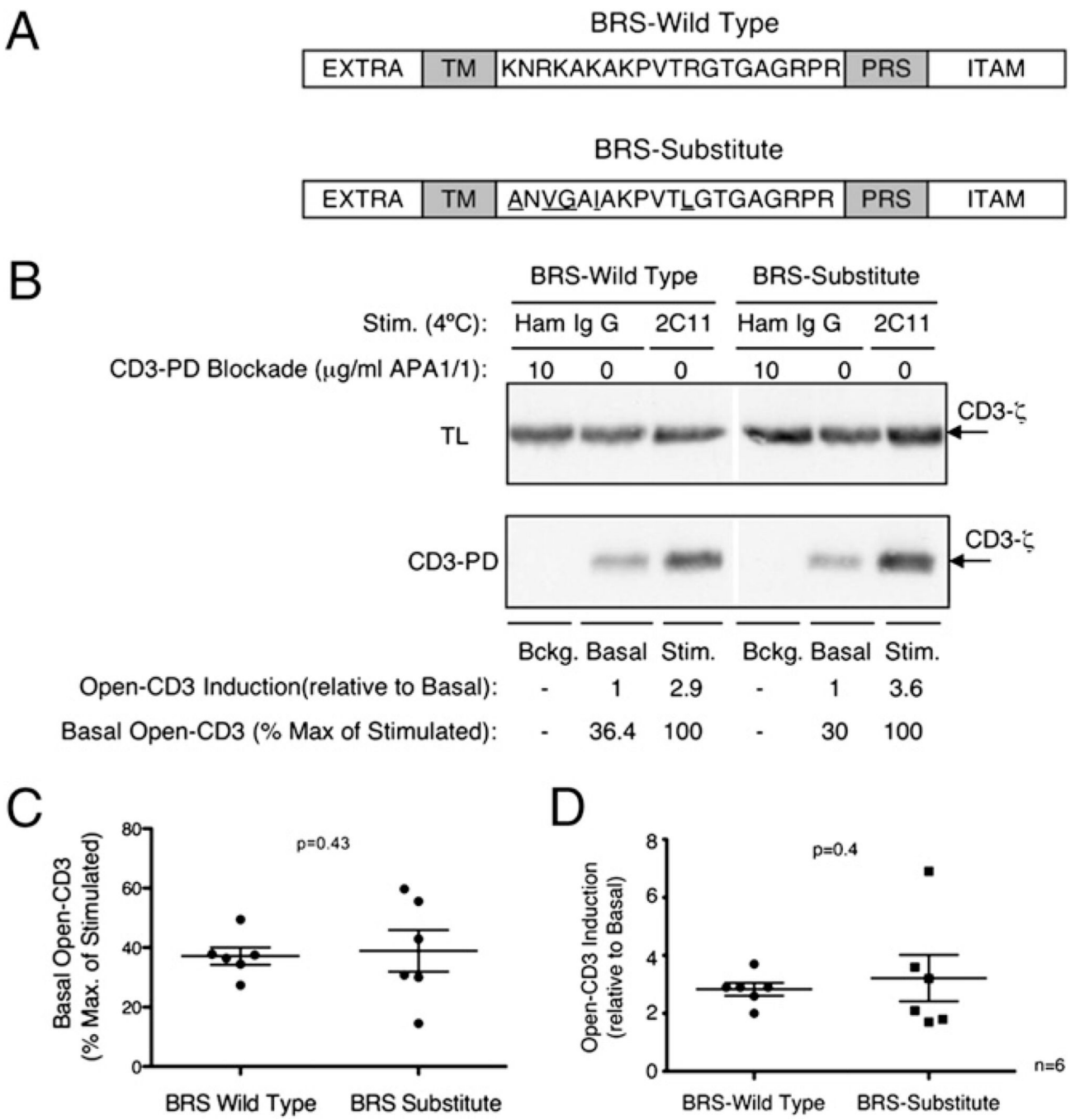

FIGURE 6.

The CD3ε BRS is not required to conceal the PRS in absence of TCR–CD3 engagement. *A*, Schematic representation of the amino acid sequence of murine CD3ε and its domains with either the WT (*top*) or the substitute (*bottom*) BRS sequence (EXTRA, extracellular; TM, transmembrane; BRS, basic amino acid-rich stretch; PRS, proline-rich sequence; ITAM, immunoreceptor tyrosine-based activation motif). *B*, Thymocytes from mice transgenic for either CD3ε BRS WT or BRS-Substitute were lysed and subjected to the CD3-PD assay to assess background, basal, and 2C11-stimulated open-CD3 levels as previously described. *C* and *D*, Values of basal open-CD3 as a percent maximum of 2C11 stimulation (*C*) and of open-CD3 induction achieved by 2C11 stimulation over basal (*D*) are plotted for six

NIH-PA Author Manuscript

NIH-PA Author Manuscript

NIH-PA Author Manuscript

independent experiments. The mean ± SE is displayed representing the amount of open-CD3 found in thymocytes from each mouse type. Paired *t* tests were run to calculate *p* values, which indicate that basal and open-CD3 induction in CD3ε BRS WT versus BRS-Substitute thymocytes are not statistically different.

NIH-PA Author Manuscript

NIH-PA Author Manuscript

NIH-PA Author Manuscript

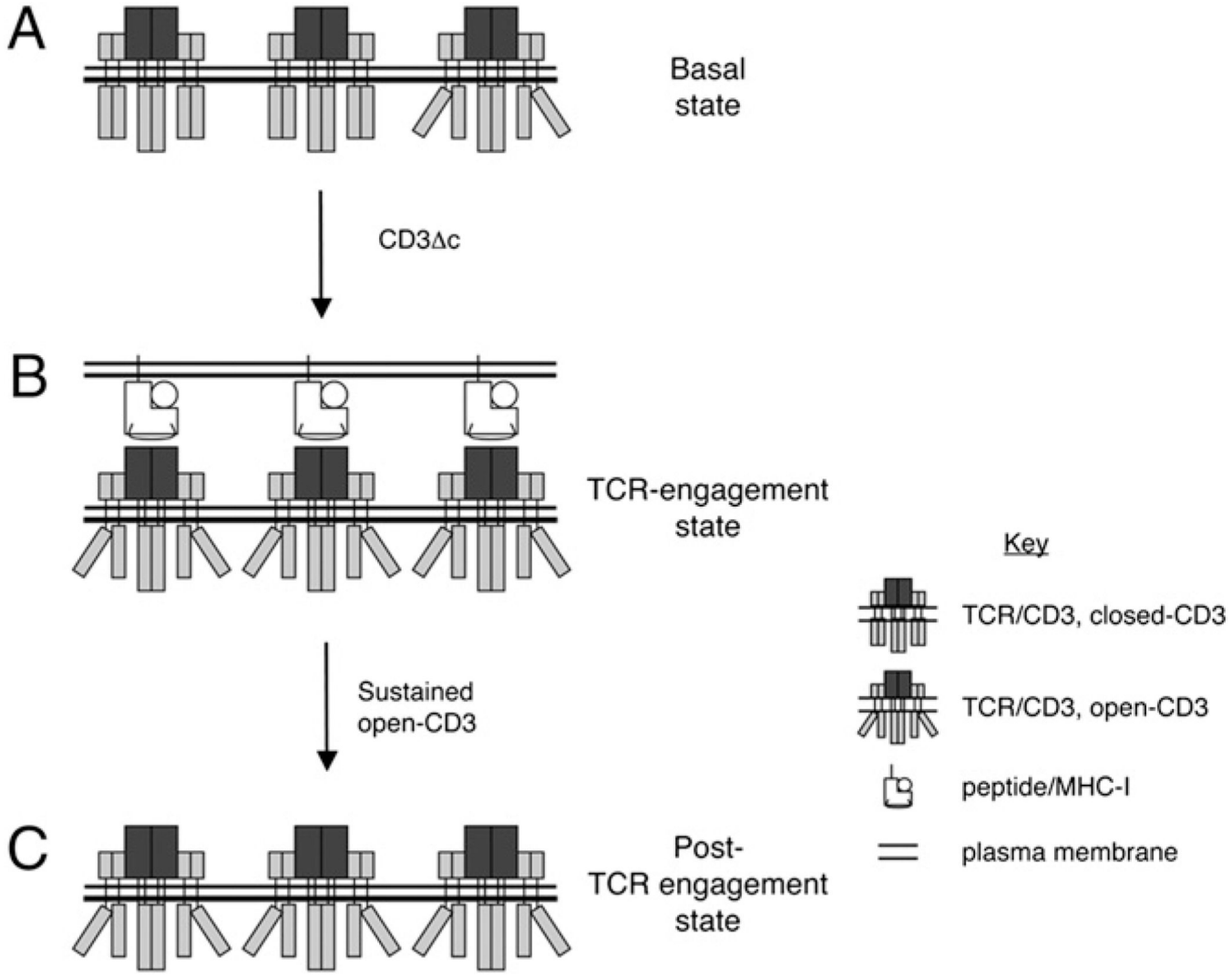

FIGURE 7.

Model of the regulation of PRS accessibility in thymocytes. Based on the accessibility of the CD3ε PRS to interact with the SH3.1 domain of Nck, we distinguish two conformations for the CD3 complex: closed-CD3 is inaccessible, whereas open-CD3 is accessible. CD3Δc is defined as the transition between these two alternative conformations (*A, B*). *A*, In a basal state characterized by the absence of TCR engagement with pMHC ligands, there is a minimum but positive amount of open-CD3. *B*, When TCR–CD3 is engaged by pMHC ligands expressed by APCs, CD3Δc increases the level of open-CD3. *C*, This new level of open-CD3 can endure beyond receptor engagement. Possible mechanistic and functional roles for this series of events are discussed in the text.